

7-1-1978

Measurements of orbit-lattice coupling of Er and Dy impurities in Ag and Al hosts

S. A. Dodds

University of California, Los Angeles

Jeff Sanny

Loyola Marymount University, jeff.sanny@lmu.edu

Repository Citation

Dodds, S. A. and Sanny, Jeff, "Measurements of orbit-lattice coupling of Er and Dy impurities in Ag and Al hosts" (1978). *Physics Faculty Works*. 38.

http://digitalcommons.lmu.edu/phys_fac/38

Recommended Citation

S. Dodds, and J. Sanny, "Measurements of orbit-lattice coupling of Er and Dy impurities in Ag and Al hosts," *Phys. Rev. B* 18, 39-44 (1978).

Measurements of orbit-lattice coupling of Er and Dy impurities in Ag and Al hosts

S. A. Dodds and J. Sanny

Department of Physics, University of California, Los Angeles, California 90024

(Received 14 February 1977)

The magnetic resonance of dilute Dy and Er impurities has been observed in thin polycrystalline Al and Ag films on two different substrates. The films are deposited at room temperature, and the measurements are made at liquid-helium temperatures. During cooling, the difference in thermal contraction between film and substrate produces an effectively uniaxial strain in the film. This results in an anisotropic g value, which we have used to obtain lower limits on the orbit-lattice coupling coefficient for these systems. We find values for $V(\Gamma_{3g}, 2)$ from 600 to 2000 cm^{-1} , somewhat smaller than observed in insulators, but of the same order of magnitude. Measurements on substrates with different thermal contractions indicate that all of the expected strain is present in these films, contrary to previous measurements on Ag:Er films grown on NaCl surfaces.

I. INTRODUCTION

The relaxation toward thermal equilibrium of an excited impurity spin in an insulating host requires transfer of energy from the spin to the host lattice. The primary cause of this energy transfer is phonon modulation of the host-crystal electric field at the impurity site.¹ It is possible to estimate the strength of the spin-phonon coupling by applying uniaxial stress to the host crystal and measuring the resulting changes in the impurity ESR spectrum. In favorable cases, the static orbit-lattice coupling parameters measured in this way give a satisfactory account of the observed phonon-driven spin-relaxation behavior.^{1,2}

Spin-phonon coupling should be present in a metallic host, but the spins can also transfer energy to the host lattice by way of their exchange coupling to the conduction electrons. In most metals, the conduction electrons dominate the spin relaxation, leading to the characteristic linear dependence of ESR linewidth on temperature.^{3,4} Static crystal-field effects in metallic hosts are well known,^{1,2} especially for rare-earth impurities, suggesting that the state of the impurity is not substantially different from what it would be in an insulator. It is therefore of interest to estimate the orbit-lattice coupling strength, in order to determine if this aspect of the host-impurity interaction is greatly changed in a metallic host.

Since phonon-driven spin relaxation has not been identified in most metallic-host-impurity systems, the only way to estimate the orbit-lattice coupling strength is by means of uniaxial stress experiments. The strains needed to cause reasonable changes in the ESR spectrum are rather large, on the order of 1%. Bulk metal crystals will plastically deform before such large strains are achieved. It is known, however, that thin films may exhibit pure elastic behavior for strains as large as 5%.⁵ This fact was recently exploited to measure the

strain dependence of the crystal field acting on Er in Ag.⁶ That work was sufficient to show that the orbit-lattice coupling is measurable in a thin film. Unfortunately, poor adhesion of the films to the substrate caused the actual strain to be nonuniform and less than the expected strain. As a result, it was only possible to determine a lower limit for the orbit-lattice coupling. The present work follows the methods of Ref. 6, but the use of two different types of substrate allows us to be sure that the actual strain in the film is the same as the expected strain. Unlike the work of Ref. 6, the films used here are not single crystals. Because of this, we are only able to find a lower limit for the coupling parameter, but the limit is substantially larger than that previously obtained. The coupling of the ions to the lattice strain is, in fact, large enough to suggest that phonon relaxation of spins may be important in some metallic hosts.

We outline the theory of ion-lattice coupling and discuss the generalizations appropriate for our polycrystalline specimens in Sec. II. Section III describes the film preparation, ESR measurements, and results. Section IV summarizes and interprets our findings.

II. THEORETICAL CONSIDERATIONS

In the experiments described here, a thin film of rare-earth doped metal is deposited on an insulating substrate at room temperature. Subsequent ESR measurements are carried out at helium temperatures. Because of the large difference between deposition and measurement temperatures, the differential contraction of film and substrate produces a substantial uniform strain in the film. The ESR signal then exhibits a g value which depends on the angle between the surface normal and the applied field.

The magnitude of the strain at the film-substrate interface is given by

TABLE I. Integrated thermal contractions from 300 to 0 K.

Substance	$\Delta L/L$	Reference
Aluminum	-41.5×10^{-4}	a
Silver	-41.0×10^{-4}	a
Fused quartz	$+0.7 \times 10^{-4}$	a
Polymethylmethacrylate (Plexiglass)	-115.0×10^{-4}	b

^a *American Institute of Physics Handbook*, 3rd ed. (McGraw-Hill, New York, 1972).

^b A. Goldsmith, T. E. Waterman, and H. J. Hirschhorn, *Handbook of Thermophysical Properties of Solid Materials* (Macmillan, New York, 1961).

$$\epsilon_{xx} = \epsilon_{yy} = (\Delta L/L)_{\text{film}} - (\Delta L/L)_{\text{substrate}}, \quad (1)$$

where $\Delta L/L$ is the integrated thermal contraction from room to helium temperatures. The values we have used are given in Table I. The strains given by Eq. (1) are in the plane of the substrate. In order to calculate the ESR response, we also need the resultant strain in the direction normal to the substrate. It will eventually be convenient to express the strains in a coordinate system oriented along the (cubic) crystal axes, not necessarily parallel to the substrate axes.

If we assume that the elastic constants of the film are the same as those of the bulk, and hence known, the resulting crystal strains can be calculated by standard methods.⁷ Since the substrate cannot exert forces on the top of the film, the stress tensor takes the form

$$\sigma = \begin{pmatrix} \sigma_{xx} & \sigma_{xy} & 0 \\ \sigma_{xy} & \sigma_{yy} & 0 \\ 0 & 0 & 0 \end{pmatrix} \quad (2)$$

in the substrate coordinate system. Note that since the crystal may have any orientation, $\sigma_{xx} \neq \sigma_{yy}$ in general. We can simplify the strain tensor by noting that the thermal contraction of the substrate is isotropic, so the length of any line in the $x-y$ plane must be independent of orientation. The resulting strain, again referred to the substrate axes, is of the form,

$$\epsilon = \begin{pmatrix} \epsilon_{xx} & 0 & \epsilon_{xz} \\ 0 & \epsilon_{xx} & \epsilon_{yz} \\ \epsilon_{xz} & \epsilon_{yz} & \epsilon_{zz} \end{pmatrix}. \quad (3)$$

The applied stress and the resulting strain are connected by Hooke's law

$$\epsilon_{ij} = S_{ijkl} \sigma_{kl}, \quad (4)$$

where repeated indices are summed. The elastic compliance tensor S_{ijkl} has only three independent

components for a cubic crystal. Equation (4) represents six independent equations linking the six unknown stresses and strains in Eqs. (2) and (3) to the known ϵ_{xx} strain given by Eq. (1). Since the strains are needed with respect to the crystallite axes within the film, it is convenient to transform ϵ and σ to the crystallite axis system before solving (4) for the strains. This also has the advantage of simplifying the form of S .

Once the thermally induced strain has been calculated for the desired crystallite orientation, the effect on the ESR can be found by treating the strain as a perturbation on the cubic crystal field. The ions considered here, Dy and Er, have a Γ_7 doublet lowest state and a Γ_8 quadruplet excited state. The perturbation on these levels can be described by the orbit-lattice coupling Hamiltonian¹

$$H_{OL} = \sum_{m,l} V(\Gamma_{3g}, l) C(\Gamma_{3g} m, l) \epsilon(\Gamma_{3g}, m) + \sum_{m,l} V(\Gamma_{5g}, l) C(\Gamma_{5g} m, l) \epsilon(\Gamma_{5g}, m) (-1)^m. \quad (5)$$

The Hamiltonian has been written in terms of the irreducible representations of the cubic group, with m denoting a particular subvector. The $C(\Gamma_{ig} m, l)$ are appropriate linear combinations of spherical harmonics acting on the $4f$ electron coordinates and the $\epsilon(\Gamma_{ig}, m)$ are similar combinations of strain amplitudes.¹ $V(\Gamma_{ig}, l)$ is the coupling coefficient, and the index l takes on the values 2, 4, and 6 for the rare earths. The number of independent $V(\Gamma_{ig}, l)$ is reduced somewhat by relations among the $V(\Gamma_{ig}, l)$ and between the $V(\Gamma_{ig}, l)$ and the cubic crystal-field coefficients,⁸ but these relations will not be needed here. The Hamiltonian [Eq. (5)] mixes the excited Γ_8 state into the Γ_7 ground state. Because of this admixture, Zeeman splitting of the Γ_7 state is found to depend on the angle between the external field and the crystal axes. The form of the angular variation, most conveniently expressed as an anisotropic g value, will depend on the nature of the applied strain through the $\epsilon(\Gamma_{ig}, m)$.

The above argument has been developed for a single crystallite subjected to an arbitrarily oriented external strain. The samples studied here are, in fact, polycrystalline, and it might appear that all strain effects will be averaged out by the random crystallite orientations. This is not the case experimentally, and the reasons can be seen relatively easily. Considering the film as macroscopically isotropic, the contraction of the substrate forces the film to expand in the direction normal to the substrate. The normal thus becomes a preferred axis, and the g value may depend on

the orientation of the field with respect to that axis.

Microscopically, the situation is somewhat more complicated and is perhaps best examined by treating a special case. Consider the $\varepsilon(\Gamma_{3g}, \theta)$ distortion given by¹

$$\varepsilon(\Gamma_{3g}, \theta) = \frac{1}{2}(2\varepsilon_{zz} - \varepsilon_{xx} - \varepsilon_{yy}), \quad (6)$$

where the strains are referred to the crystal axes. It is easy to show that the angular dependence of the g value for this strain will be given by⁶

$$g(\theta) = g + \frac{1}{2}\Delta g(3 \cos^2 \theta - 1), \quad (7)$$

where g is the undistorted g value, Δg is the amplitude of the strain-induced g shift (assumed small), and θ is the angle between the crystallite z axis and the applied field. We can also define another, experimentally observable, angle θ' between the applied field and the substrate normal. If a particular crystallite is aligned so that its [100] direction is along the substrate normal, the observed variation of the g value for that crystallite will be given by Eq. (7) with θ' replacing θ . Other crystallites will, of course, have other orientations and hence angular dependences, which will be determined by the angle between the crystallite z axis and the substrate normal, as well as the plane of rotation of the external field.

If the orientations of the crystallites are random, as we assume, and if all the crystallites had the same amount of $\varepsilon(\Gamma_{3g}, 2)$ strain, the g anisotropy would average out, producing only an inhomogeneous width. In fact the individual crystallite strains are not all the same, but depend explicitly on crystallite orientation with respect to the substrate, in such a way that the $\varepsilon(\Gamma_{3g}, 2)$ strain falls rapidly as the crystallite z axis is tilted away from the substrate normal. Since Δg is proportional to $\varepsilon(\Gamma_{3g}, 2)$, crystallites whose z axes are not well aligned will contribute progressively less to the anisotropy. The effect on the linewidth is considered below.

The detailed form of the relationship between strain and orientation follows from the solution of Eq. (4), but the result can be deduced qualitatively as follows. Consider an aligned crystallite, with z axis perpendicular to a substrate that contracts more than the film. The substrate forces contractions ε_{xx} and ε_{yy} , to which the crystal responds by expanding in the z direction. Now imagine tilting the crystal about the y axis until the z axis lies in the plane of the substrate. The extension is now along the x axis, and there is a contraction along the y and z axes. Hence, as the crystallite orientation is changed, the z -axis extension decreases smoothly to zero and then becomes a compression. Since the crystallites have

cubic symmetry, we are free to relabel the axes so that the cube axis closest to the substrate normal is the z axis, and we can see immediately that there will always be a net strain in the z direction, falling to zero as the cube axis departs from the substrate normal. The combination of strains given by Eq. (6) behaves similarly, so Δg also decreases as the crystallite z axis departs from the substrate normal. Averaging Eq. (7) over crystallite orientation, and accounting for the decrease in Δg , one finds an expression formally identical to (7), but with θ' replacing θ , and $\Delta g'$ replacing Δg :

$$g(\theta') = g + \frac{1}{2}\Delta g'(3 \cos^2 \theta' - 1). \quad (8)$$

The angular averaging has the effect of reducing Δg by about one-third for a given strain (i.e., $\Delta g' \approx \frac{1}{3}\Delta g$), the exact reduction depending on the elastic constants S_{ijkl} .

Angular dependences can also be calculated for the other terms in the Hamiltonian [Eq. (5)]. The results for the $l=2$ terms are summarized in Table II. Since there is only one preferred direction in the film, terms which depend on two angles will contribute to the inhomogeneous width, as noted below, leaving only the $(\Gamma_{3g}, 2)$ term to contribute to the g anisotropy for $l=2$. Similar but more complicated results can be derived for $l=4$ and 6.

The observed width of the resonance can arise from several mechanisms, in addition to the usual Korringa broadening. Arbilly *et al.*⁶ noted that a nonuniform $(\Gamma_{3g}, 2)$ strain in their single-crystal film would produce an anisotropic linewidth of the form

$$\Delta H = a + b(3 \cos^2 \theta' - 1), \quad (9)$$

and actually observed such a variation. For our polycrystalline samples, crystallites which have strains other than $(\Gamma_{3g}, 2)$ will contribute to the signal at various g values, as determined by their orientation. In the absence of a preferred orientation for the crystallites, the resulting linewidth will be isotropic. Crystallites which have primarily $(\Gamma_{3g}, 2)$ strains will also contribute to the in-

TABLE II. Angular dependence of the g value for various strains. The $m = \pm 1$ terms have been combined to obtain a Hermitian operator from (5).

Symmetry	Angular dependence
$(\Gamma_{3g}, 2, \theta)$	$\cos^2 \theta$
$(\Gamma_{3g}, 2, e)$	$\sin^2 \theta \cos 2\phi$
$(\Gamma_{5g}, 2, 0)$	$\sin^2 \theta \sin 2\phi$
$(\Gamma_{5g}, 2, \pm 1)$	$\sin 2\theta \cos \phi$
	$\sin 2\theta \sin \phi$

homogeneous width, but their contribution will be anisotropic. To understand the anisotropy, note that from the above argument for the g shift, we may consider the strain axes of the individual crystallites to be randomly distributed within a cone of half-angle approximately 45° , centered on the substrate normal. If the external field is now applied along the substrate normal, there will be large numbers of strain axes at each of many angles with respect to the field. Equation (7) then implies a range of g values and a substantial inhomogeneous width. When the field is oriented parallel to the substrate, there is a set of crystallites whose strain axes lie in a plane perpendicular to the field, and which, therefore, all have the same g value. The number of crystallites with strain axes at a given angle decreases rapidly as one leaves this plane, so the inhomogeneous width will be less than that for the field-normal geometry. The resulting angular dependence is not necessarily monotonic, but will be determined by the structure of the film and the relationship between strain and crystallite orientation. Given our limited knowledge of the film structure, a detailed calculation is not possible. Fortunately, this broadening mechanism can be distinguished from the macroscopic nonuniformity previously considered by making measurements on different substrates. This point is discussed more fully in Sec. III.

It is clear from the arguments above that polycrystalline material should display g anisotropy when subjected to uniaxial strain and that the form of the anisotropy is calculable. We have not attempted a quantitative calculation of $\Delta g'$ for two reasons. First, the structure of our films is not known, but there is reason to believe that it may be rather complex and may exhibit preferred crystallite orientations.⁹ Second, even if the structure were known, it would be necessary to solve Eq. (4) for each crystallite, taking into account the boundary conditions with the neighbors.¹⁰ Together, these two facts make the calculation intractable. However, if we assume that the $l=2$ terms in Eq. (5) are dominant, Table II shows that only the $(\Gamma_{3g}, 2)$ strain will contribute to the observed $\Delta g'$. We can then use the measured $\Delta g'$, and the ionic wave functions to determine a value for $V(\Gamma_{3g}, 2)$. Since $\Delta g'$ is smaller than Δg by an unknown amount, the value of $V(\Gamma_{3g}, 2)$ obtained is only a lower limit. In addition, the dominance of the $l=2$ term has been questioned for insulating hosts,² although it may be a more reasonable approximation for metals.⁶ Because of these uncertainties, the values of $V(\Gamma_{3g}, 2)$ reported in this paper may be of primary use for comparison with insulator values.

III. EXPERIMENTAL METHODS AND RESULTS

Film samples were prepared by resistive evaporation onto room-temperature fused-quartz or polymethylmethacrylate (PMMA, Plexiglass) substrates at pressures of $(1-2) \times 10^{-6}$ Torr in a diffusion-pumped system. The films studied ranged in thickness from 4000 to 6000 Å and were deposited at approximately 25 Å/sec. Thicknesses were measured by a quartz-crystal monitor during evaporation and confirmed with an optical interferometer after removal from the vacuum system. The rare-earth doping was obtained by placing weighed amounts of high-purity host material and the desired rare earth in the tungsten evaporation boat immediately before pumping down for the evaporation. Since neither Al nor Ag evaporate significantly until well above their melting points, there is ample time for the liquid alloy to be well homogenized by the stirring action of the heater current. Both Ag and Al films were made with nominal rare-earth concentrations varying from 0.2 to 2 at.%. In all cases, the residual ESR width increased with increasing nominal rare-earth concentration as expected,¹¹ but the actual values indicated concentrations smaller than nominal. The 0.2-at.% samples showed the narrowest lines consistent with good signal to noise, so most measurements were made at 0.2-at.% nominal concentration. For these samples, the linewidth indicates a concentration of approximately 0.1 at.%. As noted above, there will also be a strain-induced linewidth in these films, so it can only be concluded that the concentration is below 0.1 at.%. Loss of the rare-earth solute can probably be accounted for by the presence of residual oxygen during evaporation.

It is known¹² that strains on the order of 0.3% can occur in thin films as a result of normal film growth processes. Since we are concerned with thermally induced strains of the same order, this could seriously affect our results. Comparing the data in Tables I and III, one can see that $\Delta g'$ for any particular host-impurity system is proportional to the difference in thermal contraction of film and substrate. Also note that $\Delta g'$ changes sign when the difference in thermal contraction between film and substrate is reversed. If there were a large constant strain in the films as a result of normal film growth processes, we would not expect to observe this proportionality and sign change. We conclude that our films do not have significant growth-induced strains.

Resonance measurements were made at 9.4 GHz with the samples immersed in liquid helium. The temperature was determined by measuring the vapor pressure of the bath. In all cases, the films

TABLE III. Summary of experimental results and derived orbit-lattice coupling constants.

Alloy	Substrate	x	W^a	g	$\Delta g'$	$V(\Gamma_{3g}, 2)$ (cm^{-1})
Al:Er	quartz	-0.30	0.64 K	6.80 ± 0.02	0.33 ± 0.03	2050 ± 150
Al:Er	PMMA ^b	-0.30	0.64	6.78 ± 0.02	-0.55 ± 0.04	2000 ± 150
Al:Dy	quartz	0.53	0.44	7.59 ± 0.03	-0.54 ± 0.05	700 ± 70
Ag:Er	quartz	-0.34	0.54	6.82 ± 0.02	0.15 ± 0.02	600 ± 70
Ag:Er	PMMA	-0.34	0.54	6.85 ± 0.02	-0.22 ± 0.02	550 ± 70
Ag:Er ^c	NaCl	-0.34	0.54	6.80 ± 0.02	-0.17 ± 0.02	280 ± 30
Ag:Dy	quartz	0.53	0.44	7.67 ± 0.06	-0.69 ± 0.06	750 ± 70
MgO:Er ^d	bulk	0.71	2.39	$-13\,400 \pm 600$
CaF ₂ :Dy ^d	bulk	0.60	2.16	1800 ± 140

^a x and W are in the notation of Ref. 15.

^b Polymethylmethacrylate, Plexiglass.

^c Data from Ref. 6.

^d Data from Ref. 2.

were thick enough to exhibit the typical asymmetric metallic lineshape. The true linewidth and g value were extracted by the method of Peter *et al.*,¹³ assuming a Lorentzian lineshape. Angular variation of g value and linewidth was measured for each sample at a fixed temperature. The temperature dependence of the linewidth from 1.5 to 4.2 K was also measured for several samples. Both the slope of the linewidth versus temperature curve and the unstrained g value, deduced from fitting the data to Eq. (8), agree with the bulk values.^{11,14} This gives us considerable confidence that the rare earth is in solution. In principle, the anisotropic broadening discussed below could lead to an apparent g shift, but the effect is not large enough to be significant in our samples.

Figure 1 shows curves of g value versus angle

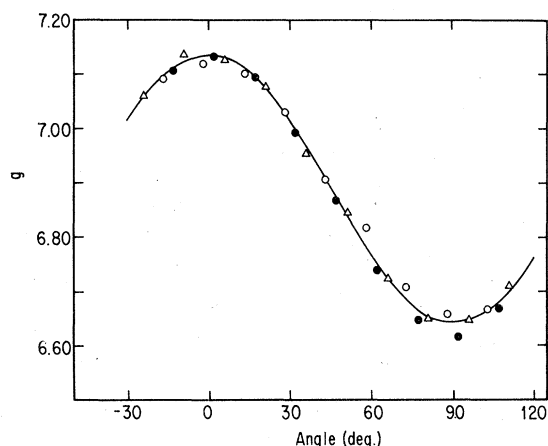


FIG. 1. Resonance g value versus-magnetic field orientation for three different Al:Er films on fused-quartz substrates, measured at 1.5 K. As discussed in the text, the Er concentration is not well known, but is less than 0.1 at.% in all three films. The angle plotted is θ' , the angle between the magnetic field and the normal to the film. The solid line is the result of fitting Eq. (8) to the data.

for the three Al:Er specimens. Fitting to Eq. (8) gives values for g and $\Delta g'$, which are listed in Table III for the various systems. The values given are the averages for several films in each case. We characterize the rare-earth wave functions by the parameters W and x ,¹⁵ which are related to the overall magnitude of the cubic crystal-field splitting and to the ratio between the fourth and sixth degree crystal-field terms, respectively. Knowing the experimental $\Delta g'$, one can then use the tabulated¹⁵ rare-earth wave functions to estimate $V(\Gamma_{3g}, 2)$. The values of W and x used are shown in Table III. They were taken from susceptibility¹⁶ and resonance¹⁷ measurements. These parameters are relatively uncertain, but any reasonable choice will lead to a value of $V(\Gamma_{3g}, 2)$ within a factor of 2 of that in Table III.

Figure 2 is a plot of linewidth versus angle for one of the Ag:Er samples. Note that the angular dependence is small and qualitatively similar to that attributed to nonuniform strain by Arbilly

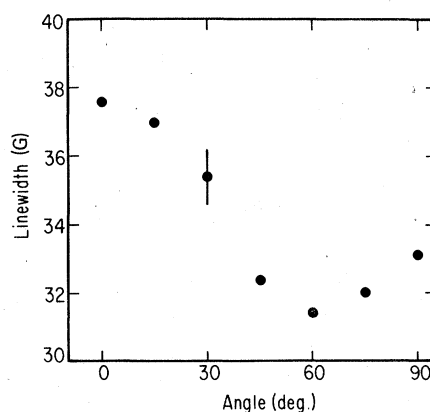


FIG. 2. Resonance linewidth versus magnetic field orientation for a Ag:0.1-at.%-Er film on fused quartz, at 1.5 K. The angle plotted is θ' , between the magnetic field and the normal to the film. The significance of the angular dependence is discussed in the text.

*et al.*⁶ However, examination of Table III indicates that the value of $V(\Gamma_{3g}, 2)$ deduced from the quartz substrate, which places the film in tension, is the same as that deduced from the PMMA substrate, which puts the film in compression. This fact leads us to conclude that these films are strongly adherent to the substrate, so that strain release does not occur, and the strain is macroscopically uniform. We attribute the observed anisotropy to the distribution of crystallite orientations, as discussed above. Linewidth anisotropy is also seen in the Al samples, although it is somewhat smaller and has a monotonic variation with angle, perhaps indicating a different film structure.

IV. CONCLUSIONS

Our primary results are summarized in Table III, where we have also given some data for insulators. To make a meaningful comparison with the insulator values, it must be recalled that the $V(\Gamma_{3g}, 2)$ values we have obtained for the metallic systems are lower limits because of the reduction of $\Delta g'$ in our polycrystalline samples. Further, the insulator measurements have been made on systems in which the phonon relaxation makes a

large contribution to the observed linewidth. This tends to pick out systems in which the phonon coupling is particularly strong. Even so, it is evident that the orbit-lattice coupling in our metallic systems is comparable to that in insulators.^{1,2} This immediately suggests that phonon relaxation, frequently observed in insulators, may also be important in appropriate metallic hosts. In fact, such processes may have already been observed for Ce in LaAs,¹⁸ and for Nd in LaRh.¹⁹

Measurements made on single-crystal films, grown in several orientations on suitable substrates, would allow considerably more detailed information to be obtained, approaching that available for insulators. It would then be possible to more adequately test models of the crystal-field and virtual-bound states in metals, and better understand the importance of spin-phonon relaxation in metallic hosts.

V. ACKNOWLEDGMENTS

We wish to acknowledge many fruitful conversations with R. Orbach. This work was supported in part by the U. S. Office of Naval Research, Contract No. N00014-75-C-0245 and by the NSF, Grant No. NSF DMR 75-19544.

¹R. Orbach and H. J. Stapleton, in *Electron Paramagnetic Resonance*, edited by S. Geschwind (Plenum, New York, 1972).

²J. M. Baker and G. Currell, *J. Phys. C* **9**, 3819 (1976).

³R. Orbach, M. Peter, and D. Shaltiel, *Arch. Sci. Geneve* **27**, 141 (1974).

⁴R. H. Taylor, *Adv. Phys.* **24**, 681 (1975).

⁵D. W. Pashley, *Proc. R. Soc. Lond. A* **255**, 218 (1960).

⁶D. Arbilly, G. Deutscher, E. Grunbaum, R. Orbach, and J. T. Suss, *Phys. Rev. B* **12**, 5068 (1975).

⁷J. F. Nye, *Physical Properties of Crystals* (Oxford, U.P., London, 1957).

⁸R. Buisson and M. Borg, *Phys. Rev. B* **1**, 3577 (1970).

⁹R. F. Bunshah, *J. Vac. Sci. Technol.* **11**, 633 (1974).

¹⁰L. D. Landau and E. M. Lifshitz, *Theory of Elasticity* (Pergamon, London, 1959), p. 40.

¹¹R. Chui, R. Orbach, and B. L. Gehman, *Phys. Rev. B* **2**, 2298 (1970); D. Dahlberg, in *Phys. Rev. B* (1977) (to be published).

¹²W. Buckel, *J. Vac. Sci. Technol.* **6**, 606 (1969).

¹³M. Peter, D. Shaltiel, J. H. Wernick, H. J. Williams, J. B. Mock, and R. C. Sherwood, *Phys. Rev.* **126**, 1395 (1962).

¹⁴C. Rettori, D. Davidov, R. Orbach, E. P. Chock, and B. Ricks, *Phys. Rev. B* **7**, 1 (1973); D. Davidov, C. Rettori, A. Dixon, K. Baberschke, E. P. Chock and R. Orbach, *Phys. Rev. B* **8**, 3563 (1973).

¹⁵K. R. Lea, M. J. M. Leask, and W. P. Wolf, *J. Phys. Chem. Solids* **23**, 1381 (1962).

¹⁶G. Williams and L. L. Hirst, *Phys. Rev.* **185**, 407 (1969).

¹⁷S. Oseroff, M. Passeggi, D. Wohlleben, and S. Schultz, *Phys. Rev. B* **15**, 1283 (1977); J. F. Siebert, S. A. Dodds, and R. H. Silsbee, *Phys. Rev. B* **14**, 4813 (1976); S. A. Dodds, thesis, (Cornell University, 1975) (unpublished).

¹⁸K. Sugawara and C. Y. Huang, *J. Phys. Soc. Jpn.* **40**, 295 (1976).

¹⁹S. A. Dodds, J. Sanny, and R. Orbach, (unpublished).